Custody Transfer and Fiscal Flow Measurement by Ultrasonic Meters

Custody Transfer and Fiscal Flow Measurement by Ultrasonic Meters

By

Alcir de Faro Orlando

Cambridge Scholars Publishing

Custody Transfer and Fiscal Flow Measurement by Ultrasonic Meters

By Alcir de Faro Orlando

This book first published 2024

Cambridge Scholars Publishing

Lady Stephenson Library, Newcastle upon Tyne, NE6 2PA, UK

British Library Cataloguing in Publication Data
A catalogue record for this book is available from the British Library

ISBN (10): 1-5275-5638-7
ISBN (13): 978-1-5275-5638-6

To my wife
Teodolinda Maria de Mello Pereira de Faro Orlando

TABLE OF CONTENTS

PREFACE

Accurate flowrate measurement is an important issue when dealing with custody transfer or fiscal measurement of water, oil and natural gas. Lower values of uncertainty of measurement have been demanded for reducing the economic impact of less reliable measurements. Ultrasonic meters have been used for being capable of making a non-intrusive accurate flowrate measurement that meets the legal metrological requirements. However, understanding the working principles is important for assuring that, with the selected meter configuration and calibrating conditions, the measurement is made accurately, thus avoiding errors that could mislead the results. Besides describing how the flowrate can be calculated from the velocity measurement, the text presents a methodology for analyzing the influence of different parameters and how to minimize it, using available information in the literature from several authors. Also, the text indicates how to monitor the measurement, thus minimizing drifting errors. Flowrate simulation under several conditions was made to help the decision of choosing the adequate meter configuration and measurement conditions for attaining a given value of uncertainty. The data used for analyzing the results were gathered from several research projects of interest to the oil and natural gas industries. The theory was used to supply addition information for interpreting results.

The book describes how to calibrate, measure and specify ultrasonic flow meters to make sure that the legal metrology requirements are met in custody transfer and fiscal applications.

The book was written for a metrologist who is in charge of specifying ultrasonic flow meters, calibrating or accurately measuring water, oil and natural gas flowrate in custody transfer and fiscal measurement applications, and must have a deep knowledge of the measurement principles and the results that can be achieved, so that the legal metrology requirements can unquestionably be met.

The Brazilian Oil and Gas Company (PETROBRAS – BRAZIL) financed several research projects in Metrology. In 1986, a methodology was developed to metrologically characterize the flowrate through porous materials to be used in oil production from wells. An experimental methodology was developed to generate enough heat to melt paraffin in oil flow through pipelines and thus supporting the cleaning operation. Then, before 2000, a system was built at PUC-Rio to test the time performance of

several oil and water level meters of, respectively, ultrasonic and capacitive types, to be used in custody transfer from storage reservoirs. As a result of the need of accurately measure flowrate for custody transfer and fiscal applications, several research projects were financed by PETROBRAS – Brazil for (a) determining the maximum time interval between two consecutive ultrasonic meter calibrations for oil and gas, (b) multiphase metering for allocation of the oil production of two neighboring production wells, flowing in the same pipeline, for government royalty taxation, (c) methodology for calibrating ultrasonic meters for oil measurement at different temperature, pressure, viscosity and flowrate values, which are different from those used during calibration by laboratories in USA and Europe. The calibration and data processing procedures were discussed with the technical staff of those laboratories.

The Brazilian Oil and Gas Company (PETROBRAS – BRAZIL) also financed the construction of a water loop at PUC-Rio – Brazil, to investigate the influence of small straight pipe lengths, upstream of the meter position, on flowrate measurement by ultrasonic clamp on type meters, to be used as a transfer meter for measuring flowrate in pipelines, when a custody transfer or fiscal meter is not available at the desired position. Two other loops were also financed, aiming, (a) measurement of water content in oil-water mixtures by speed of sound measurement, and, (b) measurement of the mass of water and oil in storage reservoirs by the vertical pressure profile.

The graduate student dissertations and theses were based on obtaining results for the financed research projects. Many conference and journal articles were published. Book chapters were written for supporting teaching and research in Metrology. Many project reports were written. PhD theses were generated in Metrology, for attaining the needs of the National Institute of Metrology, Quality and Technology (INMETRO – Brazil). Finally, course completion monographs were written by undergraduate mechanical engineering students in Metrology.

The author is indebted to Dr, William M. Kays (deceased) and Dr. Robert J. Moffat, his PhD advisers at Stanford University - USA, for having provided both the theoretical and experimental knowledge of turbulent flows, including the uncertainty analysis of measurement, which were important for writing this book.

The author is indebted to Mr. André Ferreira, MSc, a manager at PETROBRAS, for having discussed critically all projects for more than 15 years, and having trusted in the results to be obtained by our laboratory (LAME/ Pontifical Catholic University of Rio de Janeiro – Brazil).

The author is also indebted to Mr. Evemero Callegario de Mendonça, an expert in electrical instrumentation, for being responsible for assuring the

operating conditions of the experimental devices used in our laboratory, together with the data taking procedure for obtaining reliable results.

The author would like to thank the Pontifical Catholic University of Rio de Janeiro, Brazil, for having supported my activities as a researcher, lecturer and graduate work supervisor in both the Mechanical Engineering Department and Graduate Program in Metrology for more than 40 years.

Finally, the author is indebted to the National Academy of Engineering, Brazil, for having trusted in my work, electing continuously myself as one of the Directors of the Institution for about 10 years.

Alcir de Faro Orlando, 2023

CHAPTER 1

THEORETICAL BACKGROUND

1-1 Measurement principles

The fluid flowrate measurement principles in pipelines by the transit time method, as measured by ultrasonic flowmeters, are detailed in (ISO/TR 12765, 1998). Fig. 1-1 shows an L_p long acoustic path between two piezoelectric sensors 1 and 2, which are placed on the surface of an internal diameter D pipeline. When the path is tilted by a Φ angle with respect to the pipeline axis, it can be shown by Eq. (1-1) that the average axial fluid velocity $\bar{u}$ along the acoustic path is a function of the upstream t_{12} and downstream t_{21} transit times, respectively when the fluid perturbation starts from sensors 1 and 2 and reaches the other one. Fig. 1-2 shows the acoustic path projection onto the pipeline cross section.

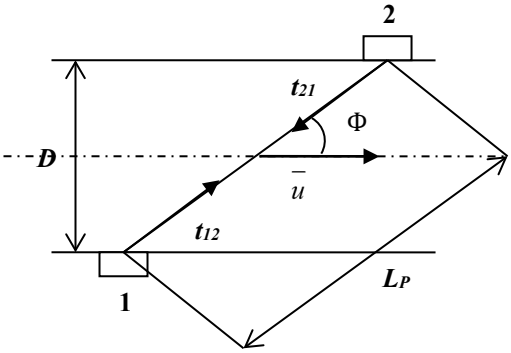

Figure 1-1: Ultrasonic flowrate measurement by the transit time method

$$\frac{1}{t_{21}} - \frac{1}{t_{12}} = \frac{2.\bar{u}.\cos(\Phi)}{L_p} \qquad (1\text{-}1)$$

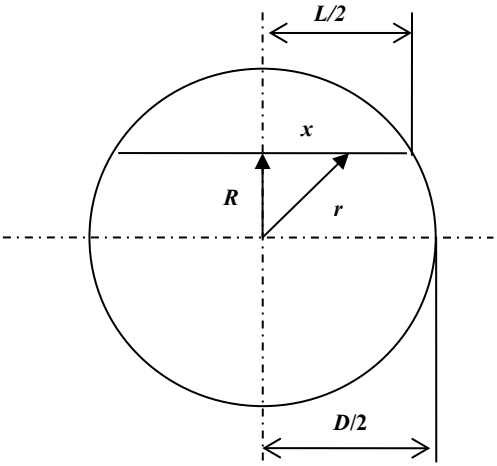

Figure 1-2: L long acoustic path in the pipeline cross section, apart R from pipeline centerline

It is possible to calculate the volumetric fluid flowrate by multiplying the pipeline cross section area and the average axial fluid velocity $\bar{u}_A$ in its cross section (average flow velocity), using the measured transit times t_{12} and t_{21}, together with Eq. (1-1) to calculate the average axial velocity $\bar{u}$ along the acoustic path. The following procedure is used with the convenient dimensionless variables (Orlando and Do Val, 2006),

$$k_h = \frac{\bar{u}_A}{\bar{u}} \tag{1-2}$$

$$a = \frac{R}{D/2} \tag{1-3}$$

$$\eta = \frac{r}{D/2} = \frac{\sqrt{x^2 + R^2}}{D/2} = \sqrt{\chi^2 + a^2} \tag{1-4}$$

$$\chi = \frac{x}{D/2} \tag{1-5}$$

$$\frac{L/2}{D/2} = \frac{\sqrt{D^2 - 4\,R^2}}{D/2} = \sqrt{1 - a^2} \tag{1-6}$$

Due to the fact that the axial fluid velocity *u(r)* is a function of the radial distance from centerline *r,* and with Eqs. (1-5) and (1-6) (Orlando and Do Val, 2006),

$$\bar{u} = \frac{1}{L/2}.\int_0^{L/2} u(r).dx = \frac{1}{\sqrt{1-a^2}}.\int_0^{\sqrt{1-a^2}} u(\chi)\,d\chi \tag{1-7}$$

$$\bar{u}_A = \frac{4}{\pi D^2}.\int_0^{D/2} 2\,\pi\,r\,u(r).dr = 2\int_0^1 \eta\,u(\eta)d\eta \tag{1-8}$$

Then, the mass flowrate $\dot{m}$ has the following expression,

$$\dot{m} = \rho\,\bar{u}_A\,(\pi D^2/4) \tag{1-9}$$

1-2 Fluid flow in smooth pipes

1-2.1 Completely developed laminar flows

In completely developed laminar flows, the velocity profile has the following expression (Schlichting, 1979)

$$\mathrm{u}(r) = 2\,\bar{u}_A\left[1-\left(\frac{r}{D/2}\right)^2\right] = 2\,\bar{u}_A\,(1-\eta^2) \tag{1-10}$$

The average axial velocities along the acoustic path $\bar{u}$ and in its cross section $\bar{u}_A$ can be obtained by integrating Eqs. (1-7) and (1-8) with the help of Eq. (1-10). Then, the shape factor k_h can be calculated by Eq. (1-2), (Orlando and Do Val, 2006), as shown by Eq. (1-11).

$$k_h = \frac{\bar{u}_A}{\bar{u}} = \frac{3}{4\,(1-a^2)} \tag{1-11}$$

Thus, the proportionality constant k_h (shape factor) between the average axial fluid velocity $\bar{u}_A$ in its cross section (average flow velocity) and the averaged axial velocity $\bar{u}$ along the acoustic path is only a function of a geometric factor *a,* not depending on Reynolds number. Table 1-1 shows the value of the proportionality constant k_h (shape factor) as a function of the geometric factor *a*.

Table 1-1: Shape factor k_h as a function of the geometric factor a, Eq. (1-11)

$a = R/(D/2)$	$k_h = \bar{u}_A/\bar{u}$
0.00	0.750
0.10	0.758
0.20	0.781
0.30	0.824
0.40	0.893
0.50	1.000
0.60	1.172
0.70	1.471
0.80	2.083
0.90	3.947

The average flow velocity $\bar{u}_A$ is equal to the average axial velocity $\bar{u}$ along the acoustic path for $a = 0.50$, for $k_h = 1$,

1-2.2 Completely developed turbulent flows

1-2.2.1 Basic concepts

Around 1930, Nikuradse obtained experimental data for several values of roughness and Reynolds number up to 3.2 x 10^6. Later on, (Schlichting, 1979) published a critical analysis of the turbulent flow theory based on experimental data. Recently, the Superpipe Facility of the Princeton University (Zagarola and Smits, 1998) obtained experimental data for values of Reynolds number in the 3.1 x 10^4 to 3.5 x 10^7 range.

Kays and Crawford (1980) made a detailed analysis of the turbulent boundary layer in the neighborhood of the pipe wall using several available three-layer velocity profile models, which usually have the following characteristics:

- A thin layer very close to the wall, usually called viscous sublayer,
- A following layer where the logarithmic law describes de velocity profile, usually called logarithmic layer,
- An outer layer that describes the behavior of most of the boundary layer and includes the pipeline centerline, characterized by a dimensionless profile.

Turbulent flows are intrinsically transient. The velocity fluctuations can vary with time around the time average velocity. Likewise, the volumetric

flow rate is time dependent. However, in many industrial applications the time average velocity stays approximately constant for long integration times, which must be experimentally determined. This class of flow has been extensively studied in the literature, and the results are used in this chapter.

The transition between the viscous sublayer and the logarithmic layer depends on the quality of the experimental data, but it seems to be only a function of the dimensionless parameter y^+, as defined by Eq. (1-22), ranging from 5 to 10.8. Van Driest (Kays and Crawford, 1980) uses a superposition function, instead of a single value. Reichardt (Kays and Crawford, 1980) suggests a single equation for the logarithmic and outer layers, outside the viscous layer.

In this chapter, the influence of the velocity profile on the shape factor determination is examined by a simple model (Kays and Crawford, 1980), although more sophisticated schemes could be eventually used. In this model, the radial distance from the centerline *r* is substituted by the radial distance from the wall *y*. Thus, a dimensionless distance from the wall can be written with the help of Eq. (1-4), (Orlando and Do Val, 2006).

$$\frac{y}{D/2} = \frac{D/2 - r}{D/2} = 1 - \frac{r}{D/2} = 1 - \sqrt{\chi^2 + a^2} \qquad (1\text{-}12)$$

A friction velocity u_τ is defined by Eq. (1-13), as a function of the shear stress at the pipe wall τ_0 and the fluid density ρ. The friction factor *f* and the Reynolds number *Re* are defined, respectively, by Eq. (1-14) and (1-15), (Orlando and Do Val, 2006).

$$u_\tau = \sqrt{\frac{\tau_0}{\rho}} \qquad (1\text{-}13)$$

$$\tau_0 = (f/4)\,\frac{\rho\,\bar{u}_A^2}{2} \qquad (1\text{-}14)$$

$$Re = \frac{\bar{u}_A\,D}{\nu} \qquad (1\text{-}15)$$

where, $\nu = \mu/\rho$ is defined as the kinematic viscosity.

Combining Eqs. (1-13) and (1-14),

$$u_\tau = \bar{u}_A \sqrt{f/8} \tag{1-16}$$

1-2.2.2 Friction coefficient

For completely developed laminar flows the literature (Zagarola and Smits, 1998) shows that,

$$f = \frac{64}{Re} \tag{1-17}$$

According to (Schlichting, 1979) and (Kays and Crawford, 1980), the universal velocity-distribution law, given by Eqs. (1-29) and (1-30), with coefficients in Table 1-3, is in excellent agreement with Nikuradse data for completely developed turbulent flows in smooth pipes, from the neighborhood of the pipe wall to the neighborhood of the pipe axis. Thus, the Karman – Nikuradse equation can be written for the friction factor,

$$\frac{1}{\sqrt{f/8}} = 2.46\, ln\left(Re\sqrt{f/8}\right) + 0.30 \tag{1-18}$$

(Zagarola and Smits, 1998), based on their experiments, proposed the following expression,

$$\frac{1}{\sqrt{f}} = 1.884\, log_{10}\left(Re\sqrt{f}\right) - 0.331 \tag{1-19}$$

Equation (1.20), developed by (Colebrook, 1939), can be used to correlate the friction factor f with Reynolds number Re and the relative roughness ε, Eq. (1-53),

$$\frac{1}{\sqrt{f}} = 1.74 - 2\, log_{10}\left[2\,\varepsilon + \frac{18.7}{Re\sqrt{f}}\right] \tag{1-20}$$

(Zagarola and Smits, 1998) used data from the Superpipe Facility of the University of Princeton to obtain Eq. (1.21)

$$\frac{1}{\sqrt{f}} = 2.065 - 1.884\, log_{10}\left[2\,\varepsilon + \frac{18.7}{Re\,\sqrt{f}}\right] \qquad (1\text{-}21)$$

Table 1-2 shows the results of the numerical calculation of the friction factor *f*, Eqs. (1-18) and (1-19), as a function of Reynolds number. Eqs. (1-20) and (1-21) were also used for comparison, assuming a relative roughness ε = 0 for smooth flows.

For Reynolds number values in the turbulent flow range, the calculated friction factor values by different references varies less than 0,0003. Equation (1-18) was used to generate reference values for being well studied by different authors in the literature. Table 1-2 shows how the friction factor varies with Reynolds number in smooth flows, using Eqs. (1-18), (1-19), (1-20) and (1-21). Those values are graphically shown in Fig. 1-3.

It can be observed that the difference between the calculated friction factor values by those equations is small.

Table 1-2: Friction Factor as a function of Reynolds number calculated by different equations for smooth flows.

Re/1000	FRICTION FACTOR FOR SMOOTH FLOWS			
	Equation			
	(1-18)	(1-19)	(1-20)	(1-21)
30	0.0234	0.0232	0.0235	0.0232
40	0.0219	0.0218	0.0220	0.0218
50	0.0208	0.0208	0.0209	0.0208
60	0.0200	0.0200	0.0201	0.0200
70	0.0193	0.0194	0.0194	0.0194
80	0.0188	0.0189	0.0189	0.0189
90	0.0183	0.0184	0.0184	0.0184
100	0.0179	0.0180	0.0180	0.0180
110	0.0176	0.0177	0.0177	0.0177
120	0.0173	0.0174	0.0173	0.0174
130	0.0170	0.0171	0.0171	0.0171
140	0.0167	0.0169	0.0168	0.0169
150	0.0165	0.0167	0.0166	0.0167
160	0.0163	0.0165	0.0164	0.0165
170	0.0161	0.0163	0.0162	0.0163
180	0.0159	0.0161	0.0160	0.0161
190	0.0158	0.0159	0.0158	0.0160
200	0.0156	0.0158	0.0157	0.0158
300	0.0144	0.0147	0.0145	0.0147
400	0.0137	0.0139	0.0137	0.0139
500	0.0131	0.0134	0.0132	0.0134
600	0.0127	0.0130	0.0127	0.0130
700	0.0124	0.0126	0.0124	0.0127
800	0.0121	0.0124	0.0121	0.0124
900	0.0118	0.0121	0.0119	0.0121
1,000	0.0116	0.0119	0.0117	0.0119

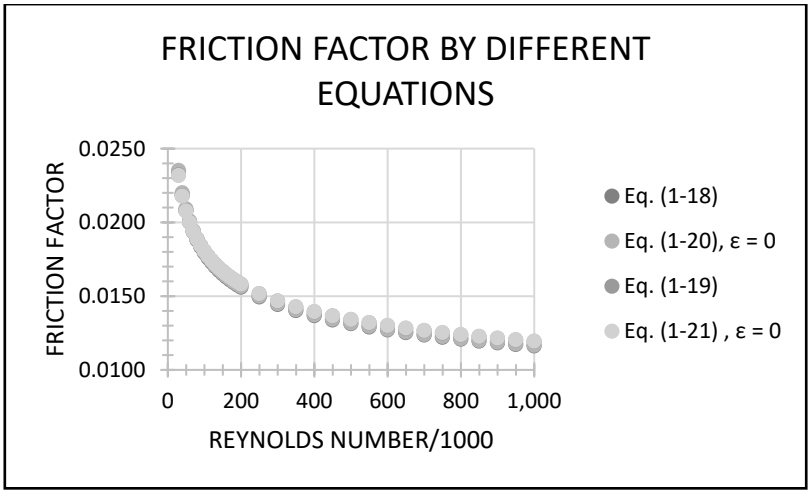

Figure 1-3: Friction Factor as a function of Reynolds number calculated by different equations, considering smooth flows (ε = 0), from Table 1-2.

1-2.2.3 Shape factor calculated by velocity profiles

The shape factor k_h is defined, Eq. (1-2), as the ratio between the average flow velocity $\bar{u}_A$ and the average axial velocity along the acoustic path $\bar{u}$.

Due to the fact that the friction factor *f* is only a function of Reynolds number *Re* in Eq. (1-18), the friction velocity u_τ in Eq. (1-16), is also only a function of Reynolds number *Re.* Using Eqs. (1-12) and (1-16), (Orlando and Do Val, 2006),

$$y^+ = \frac{y\,u_\tau}{\nu} = A^+\left[1 - \frac{r}{D/2}\right] = A^+\left[1 - \sqrt{\chi^2 + a^2}\right] \tag{1-22}$$

$$u^+ = \frac{u}{u_\tau} \tag{1-23}$$

$$A^+ = \frac{(D/2)\,u_\tau}{\nu} = \frac{1}{2}\,\frac{D\,\bar{u}_A\sqrt{f/8}}{\nu} = \frac{Re\sqrt{f/8}}{2} \tag{1-24}$$

The dimensionless parameter $\bar{u}^+$ in Eq. (1-25) can be calculated using Eqs. (1-7) and (1-16), (Orlando and Do Val, 2006),

$$\bar{u}^+ = \frac{\bar{u}}{u_\tau} = \frac{\bar{u}}{\bar{u}_A\sqrt{f/8}} = \frac{1}{k_h\sqrt{f/8}} = \frac{1}{\sqrt{1-a^2}} \cdot \int_0^{\sqrt{1-a^2}} u^+(\chi)\, d\chi \tag{1-25}$$

With the following boundary conditions,

$$y^+ = A^+(1-a) \quad for \quad \chi = 0 \tag{1-26}$$

$$y^+ = 10.8 \quad for \quad \chi = \sqrt{(1-10.8/A^+)^2 - a^2} \tag{1-27}$$

$$y^+ = 0 \quad for \quad \chi = \sqrt{1-a^2} \tag{1-28}$$

together with the following two layer velocity profile model (Schlichting, 1979) for smooth pipe flows and (Orlando and Do Val, 2006),

$$u^+ = y^+ \quad for \quad 0 \le y^+ \le A^+_{shift} \tag{1-29}$$

$$u^+ = A\ \ln(y^+) + B \quad for \quad A^+_{shift} \le y^+ \le A^+ \tag{1-30}$$

where, A^+_{shift} is the critical value of y^+, for which the velocity profile given by Eq. (1-29) intercepts the velocity profile given by Eq. (1-30), determining the validity range for each equation. (Kays and Crawford, 1980) suggest a value of $A^+_{shift} = 10.8$, based on the analysis of the available experimental data, which approximately coincides with (Schlichting, 1979).

The crossing point of the equations can be calculated by solving Eqs. (1-29) and (1-30), using coefficients of Table 1-3. This results is $A^+_{shift} = 11.6$ for Nikuradse equation, and $A^+_{shift} = 11{,}8$ for (Zagarola and Smits, 1998).

The acoustic path intercepts the pipe axis

When the acoustic path intercepts the pipe axis, $a = 0$ ($R = 0$), Eq. (1-22) results in Eq. (1.31), together with its derivative, Eq. (1-32),

$$y^+ = A^+ (1 - \chi) \tag{1-31}$$

$$dy^+ = -A^+ \, d\chi \tag{1-32}$$

Changing variables, together with the integration limits, $y^+ = A^+$ for $\chi = 0$, and $y^+ = 0$ for $\chi = 1$, Eq. (1-25) can be written as Eqs. (1-33), (1-34) and (1-35), when using the velocity profile model, Eqs. (1-29) and (1-30),

$$\bar{u}^+ = \frac{1}{A^+} \int_0^{A^+} u^+ \, dy^+ \tag{1-33}$$

$$\bar{u}^+ = \frac{1}{A^+} \int_0^{A^+_{shift}} y^+ \, dy^+ + \frac{1}{A^+} \int_{A^+_{shift}}^{A^+} [A \, ln(y^+) + B] \, dy^+ \tag{1-34}$$

$$\bar{u}^+ = \frac{1}{A^+} \left[INT_1 + A \, INT_2 + B \, INT_3 \right] \tag{1-35}$$

$$INT_1 = \left[\frac{\left(A^+_{shift}\right)^2}{2} \right] \tag{1-36}$$

$$INT_2 = \left[A^+ \, ln(A^+) - A^+ \right] - \left[A^+_{shift} \, ln\left(A^+_{shift}\right) - A^+_{shift} \right] \tag{1-37}$$

$$INT_3 = \left[A^+ - A^+_{shift} \right] \tag{1-38}$$

$$C = \left[\frac{\left(A^+_{shift}\right)^2}{2} \right] - A \left[A^+_{shift} \, ln\left(A^+_{shift}\right) - A^+_{shift} \right] - B \, A^+_{shift} \tag{1-39}$$

$$\bar{u}^+ = \left[A\ ln(A^+) + (B - A) + \frac{C}{A^+}\right] \tag{1-40}$$

$$\frac{1}{k_h} = \bar{u}^+ \sqrt{f/8} = \left[A\ ln(A^+) + (B - A) + \frac{C}{A^+}\right] \sqrt{f/8} \tag{1-41}$$

$$A^+ = \frac{Re\sqrt{f/8}}{2} \tag{1-24}$$

For comparison purposes, the shape factor coefficient C, in Eq. (1.39), was calculated and shown in Tab. 1.3 for the Karman-Nikuradse velocity profile as a function of A^+_{shift}, the crossing point between Eqs. (1-29) and (1-30).

Table 1-3: Karman Nikuradse velocity profile parameters for smooth pipe flows, to be used in Eq. (1-30), A^+_{shift}=10.8.

Parameters		Fiction Factor	Eq. (1-39)
A	B	*f*	C
2.5	5.5	Eq. (1-18)	21.0723 – 10.8 B

For the Karman – Nikuradse profile, specified in Table 1-3 and Eq. (1-24), Eq. (1-41) becomes,

$$\frac{1}{k_h} = \bar{u}^+ \sqrt{f/8} = \left[2.5\ ln\left(\frac{Re\sqrt{f/8}}{2}\right) + 3 - \frac{76.655}{Re\sqrt{f/8}}\right] \sqrt{f/8} \tag{1-42}$$

Equation (1-42) shows that the shape factor k_h for completely developed turbulent flows is only a function of Reynolds number *Re,* since the friction factor *f*, in Eq. (1-18), is also a function of Reynolds number *Re*. For each Reynolds number *Re* value in the 30,000 to 1,000,000 range, the friction factor *f* is calculated by Eq. (1-18). Then, A^+, $\bar{u}^+$ and k_h are, respectively, calculated by Eqs. (1-24), (1-40) and (1-41). Table 1-4 shows that the C/A^+

term is very small and can be neglected in Eq. (1-41). This means that inaccuracies in determining A^+_{shift} are not important for calculating C in Eq. (1-39). Therefore, as a good approximation, Eq. (1-42) can be written as,

$$\frac{1}{k_h} = \bar{u}^+ \sqrt{f/8} = \left[2.5\, ln\left(\frac{Re\sqrt{f/8}}{2} \right) + 3 \right] \sqrt{f/8} \qquad (1.43)$$

Table 1-4: Shape factor k_h as a function of Reynolds number when the acoustic path intercepts the pipe axis (a = 0), $A^+_{shift} = 10.8$.

Re/1000	f	A^+	A	B	C/A$^+$	$\bar{u}^+$	k_h
30	0.0234	811	2.500	5.500	-0.047	19.700	0.938
40	0.0219	1047	2.500	5.500	-0.037	20.347	0.939
50	0.0208	1276	2.500	5.500	-0.030	20.848	0.940
60	0.0200	1500	2.500	5.500	-0.026	21.258	0.941
70	0.0193	1721	2.500	5.500	-0.022	21.605	0.941
80	0.0188	1939	2.500	5.500	-0.020	21.905	0.942
90	0.0183	2155	2.500	5.500	-0.018	22.171	0.942
100	0.0179	2368	2.500	5.500	-0.016	22.408	0.942
110	0.0176	2579	2.500	5.500	-0.015	22.623	0.943
120	0.0173	2788	2.500	5.500	-0.014	22.819	0.943
130	0.0170	2996	2.500	5.500	-0.013	23.000	0.943
140	0.0167	3202	2.500	5.500	-0.012	23.167	0.944
150	0.0165	3407	2.500	5.500	-0.011	23.323	0.944
160	0.0163	3611	2.500	5.500	-0.011	23.469	0.944
170	0.0161	3813	2.500	5.500	-0.010	23.606	0.944
180	0.0159	4015	2.500	5.500	-0.010	23.735	0.945
190	0.0158	4215	2.500	5.500	-0.009	23.857	0.945
200	0.0156	4415	2.500	5.500	-0.009	23.973	0.945
300	0.0144	6369	2.500	5.500	-0.006	24.892	0.946
400	0.0137	8266	2.500	5.500	-0.005	25.545	0.947
500	0.0131	10124	2.500	5.500	-0.004	26.053	0.948
600	0.0127	11952	2.500	5.500	-0.003	26.468	0.948
700	0.0124	13754	2.500	5.500	-0.003	26.820	0.949
800	0.0121	15536	2.500	5.500	-0.002	27.125	0.949
900	0.0118	17300	2.500	5.500	-0.002	27.394	0.950
1,000	0.0116	19049	2.500	5.500	-0.002	27.635	0.950

In Tab. 1-4 different parameters are calculated by Eqs. (1-24), (1-39), (1-40) and (1-41), using Tables 1-2 and 1-3, for the Karman-Nikuradse velocity profile in smooth flows.

The acoustic path does not intercept the pipe axis

Table 1-5: Shape factor k_h as a function of Reynolds number when the acoustic path does not intercept the pipe axis (a ≠ 0) $A^+_{shift} = 10.8$,

Shape factor k_h					
Re/1000	Geometric factor a				
	0.1	0.3	0.5	0.7	0.9
30	0.941	0.958	0.992	1.059	1.261
40	0.942	0.958	0.991	1.055	1.245
50	0.943	0.959	0.991	1.052	1.234
60	0.943	0.959	0.990	1.050	1.226
70	0.944	0.959	0.990	1.049	1.220
80	0.944	0.959	0.990	1.047	1.214
90	0.945	0.960	0.989	1.046	1.210
100	0.945	0.960	0.989	1.046	1.207
110	0.945	0.960	0.989	1.045	1.203
120	0.945	0.960	0.989	1.044	1.201
130	0.946	0.960	0.989	1.043	1.198
140	0.946	0.960	0.989	1.043	1.196
150	0.946	0.961	0.989	1.042	1.194
160	0.946	0.961	0.989	1.042	1.192
170	0.947	0.961	0.989	1.042	1.190
180	0.947	0.961	0.989	1.041	1.189
190	0.947	0.961	0.989	1.041	1.187
200	0.947	0.961	0.988	1.040	1.186
300	0.948	0.962	0.988	1.038	1.176
400	0.949	0.962	0.988	1.036	1.169
500	0.950	0.963	0.988	1.035	1.165
600	0.950	0.963	0.988	1.034	1.161
700	0.951	0.963	0.988	1.033	1.158
800	0.951	0.964	0.988	1.033	1.156
900	0.951	0.964	0.988	1.032	1.153
1,000	0.952	0.964	0.988	1.032	1.152

In Tab. 1-5 the shape factor k_h was calculated by numerically integrating Eq. (1.25) with data in Tables. 1.2 and 1.3, and Eqs. (1.29) and (1.30). Boundary conditions Eqs. (1.26), (1.27) and (1.28).

When the acoustic path does not intercept de pipe axis ($a \neq 0$), the same procedure is used for calculating A^{+}. However, $\bar{u}^{+}$ is calculated by numerically integrating Eq. (1-25), with the relationship between y^{+} and χ given by Eq. (1-22). Then the shape factor k_h is calculated as shown by Eq. (1-25). Fig. 1-4 and Table 1-5 shows the results for the Karman – Nikuradse profile, Table 1-3. It can be observed that the smallest shape factor k_h variation with Reynols number is obtained in the $0.4 < \boldsymbol{a} < 0.5$ range. When the acoustic path approaches the wall (a approaches 1) the variation becomes higher.

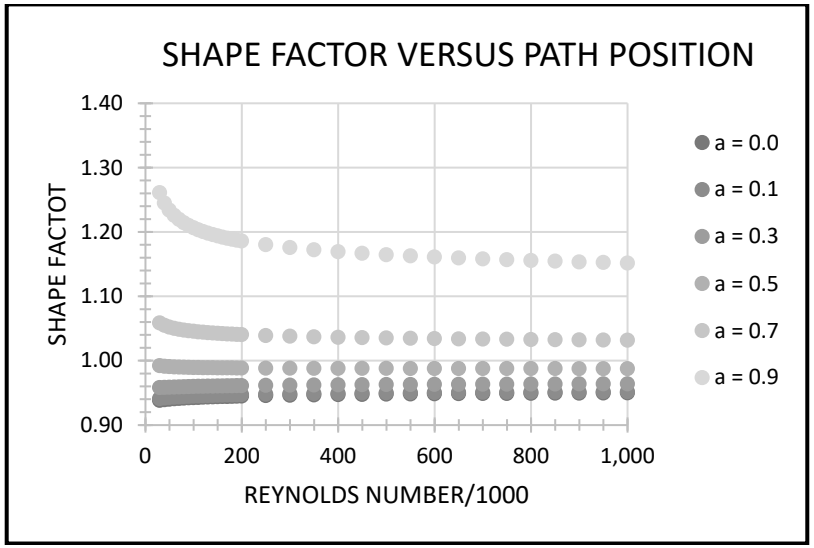

Figure 1-4: Shape factor calculated for different acoustic path positions, Karman Nikuradse profile for smooth flows, Table 1-5

1-2.2.4 Analysis of shape factor models

The accuracy of the ultrasonic flowmeter performance simulation depends fundamentally on the quality of the experimental data used for generating the velocity profile in completely developed turbulent flows.

The literature shows expressions for the velocity profile only for isothermal flows.

Furthermore, the literature does not show any velocity profile expression for developing flows that could be used in any flow condition. Therefore, errors may result if the flow is not completely developed.

Therefore, additional calibration information must be supplied to reduce the uncertainty of flowrate measurement.

The literature shows that the parabolic velocity profile seems to represent adequately the completely developed and isothermal laminar flow. On the other hand, the completely developed turbulent flow velocity profile depends on the quality of the available experimental data, resulting in flowrate measurement uncertainties that can be reduced by proper flow meter calibration.

The effective thickness of the viscous sublayer is suggested by (Kays and Crawford, 1980) to be $y^+ = 10.8$. However, Table 1-4 shows that this critical y^+ value is not important for calculating the shape factor, allowing uncertainties in its determination. The law of the wall coefficients are different from those originally proposed by Prandtl (Kays and Crawford, 1980)

$$u^+ = 2.44\ ln(y^+) + 5.0 \tag{1-44}$$

According to (Schlichting, 1979), the Karman-Nikuradse equation, Table 1-3, is in excellent agreement with Nikuradse experimental data all way through the neighborhood of the pipe wall to the neighborhood of pipe axis. This profile was thus chosen as a reference for comparison among the available profiles, following Eqs. (1-29) and (1-30).

(Zagarola and Smits, 1998), based on their experiments, proposed an expression, that reproduce the experimental data obtained by the Superpipe Facility of Princeton University to within their uncertainty of measurement. (Kays and Crawford, 1980) proposed a slight modification of Eq. (1-30) so that the derivative of the velocity profile be zero at the centerline, for symmetry reasons

$$u^+ = 2.5\ ln\left[y^+\ \frac{1.5\ (1 + r/(D/2))}{1 + 2\ (r/(D/2))^2}\right] + 5.5 \tag{1-45}$$

Finally, a simple velocity profile for smooth pipe flows has been used by several authors,